REVIEWS

Journal of Semiconductors
(2019) 40, 101302
doi: 10.1088/1674-4926/40/10/101302

Recent progress in epitaxial growth of III–V quantum-dot lasers on silicon substrate

Shujie Pan, Victoria Cao, Mengya Liao, Ying Lu, Zizhuo Liu, Mingchu Tang, Siming Chen†, Alwyn Seeds, and Huiyun Liu

Department of Electronic and Electrical Engineering, University College London, London WC1E 7JE, UK

Abstract: In the past few decades, numerous high-performance silicon (Si) photonic devices have been demonstrated. Si, as a photonic platform, has received renewed interest in recent years. Efficient Si-based III–V quantum-dot (QDs) lasers have long been a goal for semiconductor scientists because of the incomparable optical properties of III–V compounds. Although the material dissimilarity between III–V material and Si hindered the development of monolithic integrations for over 30 years, considerable breakthroughs happened in the 2000s. In this paper, we review recent progress in the epitaxial growth of various III–V QD lasers on both offcut Si substrate and on-axis Si (001) substrate. In addition, the fundamental challenges in monolithic growth will be explained together with the superior characteristics of QDs.

Key words: quantum dots; silicon photonics; epitaxial growth; semiconductor laser

Citation: S J Pan, V Cao, M Y Liao, Y Lu, Z Z Liu, M C Tang, S M Chen, A Seeds, and H Y Liu, Recent progress in epitaxial growth of III–V quantum-dot lasers on silicon substrate[J]. *J. Semicond.*, 2019, 40(10), 101302. http://doi.org/10.1088/1674-4926/40/10/101302

1. Introduction

For decades, with increasing research in the silicon (Si) microelectronics industry, the exponentially increasing complexity of integrated circuits (ICs) has been witnessed. The capabilities of interconnects have become an essential role in evaluating chip performance, especially for the very large-scale integration (VLSI). This results in the urgent demand for achieving cost-effective and high-performance integrated photonics devices. The superior properties of Si, including low-defect density, high thermal conductivity and high refractive-index contrast between Si and its native oxide i.e. SiO_2 raise the potential for scalable Si photonic integrated circuits (PICs). Thus far, the Si community has well-developed many photonics building blocks, including ultra-fast modulators[1–3], high-bandwidth detectors[4–6] and low-loss waveguides[7, 8]. Amidst this progress, the absence of an integrated laser source has impeded the full development of this field due to Si's inefficient light emission. In recent years, research groups from all over the world have succeeded in generating light on group IV platforms with the usage of competent light-emitters from group III–V[9–12]. Among these approaches, the monolithically growth of group III–V materials on Si substrate seems to be the optimum choice own to its low-cost and ease of scalability. However, the material dissimilarity between group III–V materials and Si substrates[13, 14] tends to introduce various defects that will significantly degrade devices' performance seriously. Fortunately, the well-established quantum dots (QDs) structure with its unique characteristics of defects tolerance and carrier confinement offers the possibility of practical III–V/Si integration.

Correspondence to: S M Chen, siming.chen@ucl.ac.uk
Received 29 JUNE 2019; Revised 27 JULY 2019.

This review paper began by reviewing the challenges of monolithic growth of Si-based III–V compounds. Then, the advantages of QDs for monolithic III–V/Si integration technology were discussed. Followed by our recent progress being made in achieving high-performance O-band InAs QD lasers monolithically growth of III–V QD lasers on both off cut and on-axis Si platforms.

2. Challenges in monolithic growth

Ever since the first attempt to grow GaAs thin films on Si-substrates in the 1980s[14, 15], the monolithic growth of III–Vs on Si has been pursued with little progress due to the large material dissimilarity between group III–V and group IV materials, including polar vs non-polar surfaces, lattice mismatch, and different thermal expansion coefficients. These differences tend to produce various types of defects, such as anti-phase boundaries (APBs), threading dislocations (TDs) and thermal cracks, as seen in Fig. 1, which all generate non-radiative recombination centres, and dramatically undermine the promise of III–Vs monolithically grown on Si.

The first issue shown in Fig. 1(a) is related to the formation of the APBs in III–V/Si epitaxy, which comes from the combination of polar and non-polar bonds. In practice, the Si (001) surface always contains single atomic steps, and the nucleation of the group V species on the Si surface always emerges preferentially over the group III species. Single atomic steps will induce planes of III–III and V–V bonds separately[16]. As a result, these planar defects act as nonradiative recombination centres for the optoelectronic device and affect devices' optical properties. Meanwhile, to a certain extent, they can be treated as leakage paths for electronic devices that will significantly reduce electron mobility[17, 18].

The second issue is the formation of the TDs. Compared to Si, whose lattice constant is 5.431, GaAs (5.653) has approx-

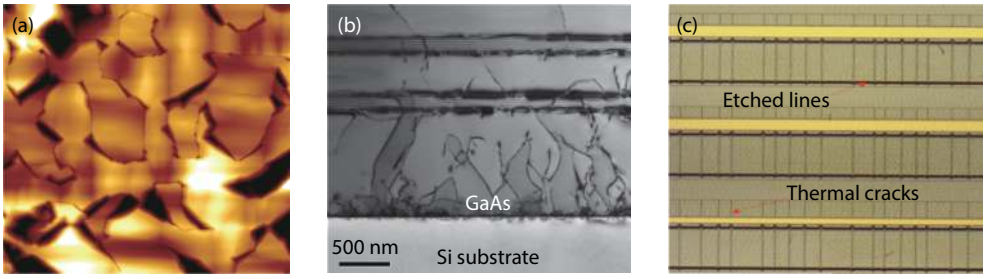

Fig. 1. (Color online) Three major issues faced in monolithic III–V/Si integration: (a) APBs, (b) TDs and (c) thermal cracks.

imately 4% lattice mismatch. This leads to continuous stress accumulation in the epilayer, and this stacked energy will be released at the pseudomorphic critical point with increasing deposition thickness. This relaxation will cause two types of dislocations: misfit dislocations and TDs. Neither of the dislocations can terminate within a crystal due to the energetic reasons; they must either stop at the edge as misfit dislocations or propagate upwards to form the TDs[19]. Consequently, the TDs tend to enhance the non-radiative recombination and eventually reduce the devices' internal efficiency as well as their lifetime[20].

The last issue is that of thermal cracks, which normally appears during the cooling-down process from high growth temperature (normally ~600 °C) to room temperature (RT). It originates from the different thermal expansion coefficient between III–V and Si material, which promotes the accumulative thermal strain in the epilayer. The strain relaxation results in cracks formed in the III–V film and this will seriously reduce the performance and the yield of the device. Moreover, it will limit the maximum achievable growth thickness of III–V compounds on Si. In addition to cracks, this thermal strain may create an extra driving force for dislocation growth and further degrade devices' performance[21].

3. Advantages of quantum dots (QDs)

After the hypothetical heterojunction structures proposed by Kroemer in 1963[22], it took seven years to realise the first double heterostructure lasers[23]. This successful demonstration reveals the necessity of carrier confinement in achieving lasing. Following this, with growing interests in quantum confined semiconductor lasers, massive progress has been made in the worldwide semiconductor laser community. By reducing the dimensionality of the active region, a quantum well (QW) structure with 1-D confinement and a quantum wire structure with 2-D confinement were achieved in 1974 and 1989 respectively[24, 25]. As those materials are well-studied, establishing a 3-D confined structure (QD) is considered as the ultimate goal due to its more significant modification of the density of states (DOSs). Even though, using the QD as the active region was proposed in 1982 by Arakawa and Sakaki[26], it was obtained only after the Stranski–Krastanow (S–K) growth method came into use in 1994[27]. This growth mode takes advantage of the strain energy resulting from the mismatched lattice constant between III–V compounds and group IV materials. With increasing thickness, the growth-material could be self-assembled into 3D islands[28]. The properties of these islands could be tuned and optimised for target applications by controlling the growth conditions such as growth temperature, growth rates, growth time and material ratios[29–31].

However, in reality, early QDs devices suffered from QD size fluctuations resulting from the inevitable self-assembly techniques[28]. For example, the inhomogeneous broadening leads to a wider spectral range along with the reduction of maximum peak gain[20]. Over the decades, optimised QDs, as well as device structures, have been pursued. With persistent efforts to improve layer structures, dots uniformity, dots density and the number of layers of dots, many predicted superior properties of QDs have been gradually exhibited, including low threshold current[28], narrow spectrum linewidth[32], large modulation bandwidth[33, 34], low relative intensity noise (RIN)[35], high efficiency and incredibly long lifetime[36]. In addition to these well-established properties, QDs have recently been widely employed as the active region for monolithic III–V/Si integration technology due to its lower sensitivity to defects results from effective carrier localisation. For example, in the QW active region, any TDs through the active region will become non-radiative recombination centres (Fig. 2(a)), leading to a significantly increased threshold or even 'killing' the device. However, in contrast, for the QD active region, one TD can only 'kill' one or a very limited number of dots, leaving the rest unaffected, and continue to contribute to optical gain[11]. Furthermore, there is a case called 'dislocation bending' in QDs material, which is presented in Fig. 2(b). For a pyramidal-shaped QD, when a TD propagates towards its base, the dislocation bending will occur if the dislocation self-energy is equal to or smaller than the strain energy released for generating a misfit dislocation[37, 38]. In this case, a piece of misfit dislocation will be generated and drift beneath the QD[39]. Moreover, the strong strain field existing in the QDs could drive away the TDs and this could further reduce the dislocation density[40].

4. QD lasers on Si substrate with off cut

In the last few years, unbelievable developments have been witnessed in Si photonics: the increasing functionality in Si-based integrated circuits (IC) and the excellent performance of most key optical components. Based on these achievements, many efforts have been devoted to fabricating efficient Si-based lasers which are indispensable to the phonics integrated circuits (PICs), and much progress has been made. In spite of that, the very first QD laser monolithically grown on Si was reported in 1999[41], and a QD laser grown on Si lase at 1.3 or 1.55 μm was not obtained until the research group from UCL achieved the first electrically pumped 1.3 μm InAs QD laser grown directly on a Si (001) substrate with 4° off-cut towards [011] plane in 2011[42]. Since then, numerous approaches have been investigated to optimise devices'

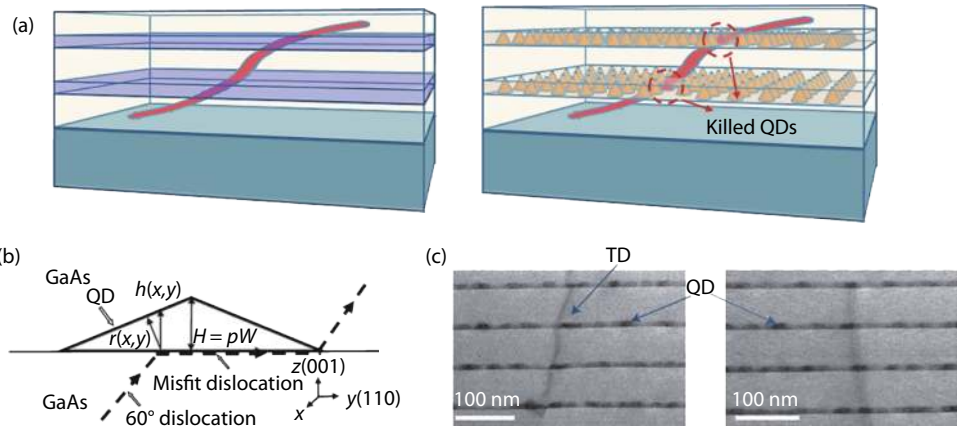

Fig. 2. (Color online) (a) Schematic illustration of the comparative interaction of threading dislocations with QWs and QDs. (b) Cross-sectional schematic description of the mechanism of dislocation bending by QDs. (c) Bright-field scanning transmission electron microscopy (TEM) images of the TDs in the QD active region[11]. Copyright © 2016, Springer Nature. With permission of Springer (c). © 2009, IEEE. Reprinted with permission from Ref. [39] (b).

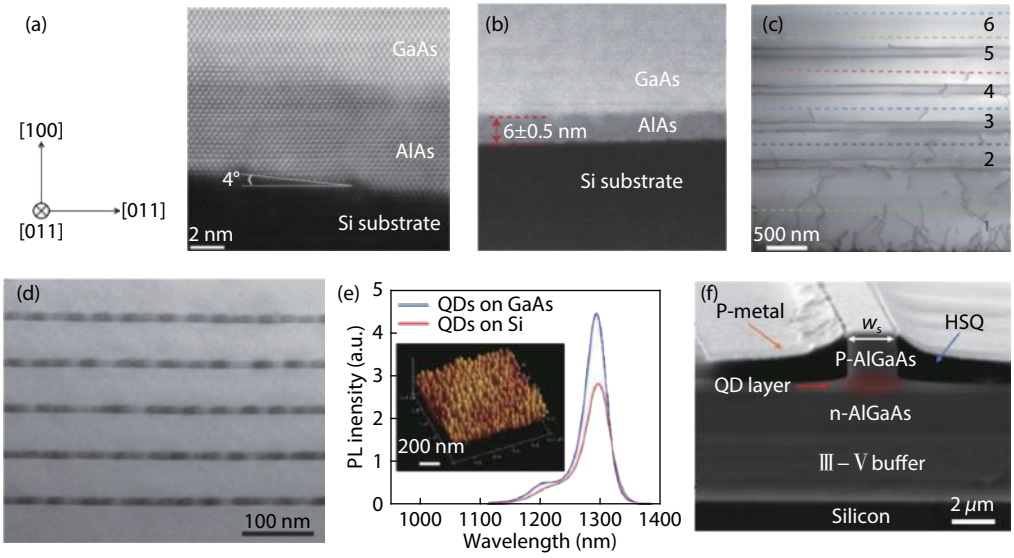

Fig. 3. (Color online) (a) Dark-field scanning TEM image of a Si substrate with 4° off-cut. (b) High resolution high-angle annular dark-field scanning TEM image of the 6 nm-thick AlAs nucleation layer between GaAs buffer layer and a Si substrate. (c) Bright-field scanning TEM image of DFLs. (d) Bright-field scanning TEM image of the QD active layers. (e) Photoluminescence (PL) spectrum of a QD active region grown on GaAs and Si. (f) Cross-sectional scanning emission microscopy (SEM) image of the fabricated RWG laser with as-cleaved facets. Copyright © 2016, Springer Nature. With permission of Springer (a–c). Reprinted with permission from Ref. [49], The Optical Society (OSA), CC BY 4.0 (d–f).

quality[43–46].

A few epitaxial growth techniques were used to minimise the impact of various defects and the general Si off cut substrate developed by the UCL group can be found in Fig. 3. The design of the 4° off-cut angle could eliminate the formation of APBs. At the initial stage, a thin AlAs nucleation layer was employed to suppress 3-D growth and provided a flat interface for the following depositions[43]. After that, a three-step growth method was introduced: a GaAs buffer layer with a thickness of 30, 170 and 800 nm grown at 350, 450 and 590 °C, respectively[18, 42]. With these techniques, most of the defects could be well confined in the first 200 nm, although the density of TDs propagating towards the active region was still as high as 1×10^9 cm^{-2}[47]. To further eliminate the TDs, the periodically strained-layer superlattices (SLSs) composed of $In_{0.18}Ga_{0.82}As$/GaAs were developed as the dislocation filter layers (DFLs)[48]. Moreover, an *in situ* thermal annealing cycle was used immediately after the growth of the SLSs which, could improve the structural and optical properties[45]. Consequently, a QD density of ~ 3.0×10^{10} cm^{-2} with relatively good quality was obtained together with a dislocation density at the order of 10^5 cm^{-2}.

In this section, a few representative off cut Si-based QD lasers fabricated using the above growth techniques will be reviewed, including the Fabry-Perot (FP) laser, the narrow-ridge-waveguide (RWG) FP laser, the distributed feedback (DFB) laser and the micro-disk laser, all on off cut Si substrate.

4.1. FP lasers on off cut Si substrate

A pioneering work was done by Chen *et al.* in 2016[11]. In this work, Si-based InAs/GaAs QD lasers grown by a solid-source molecular beam epitaxy (MBE) lasing at 1.3 μm were demonstrated. Thanks to the rigorous design and growth, a high-performance electrically pumped continuous-wave (CW) 1310 nm III–V/Si laser was achieved with remarkable proper-

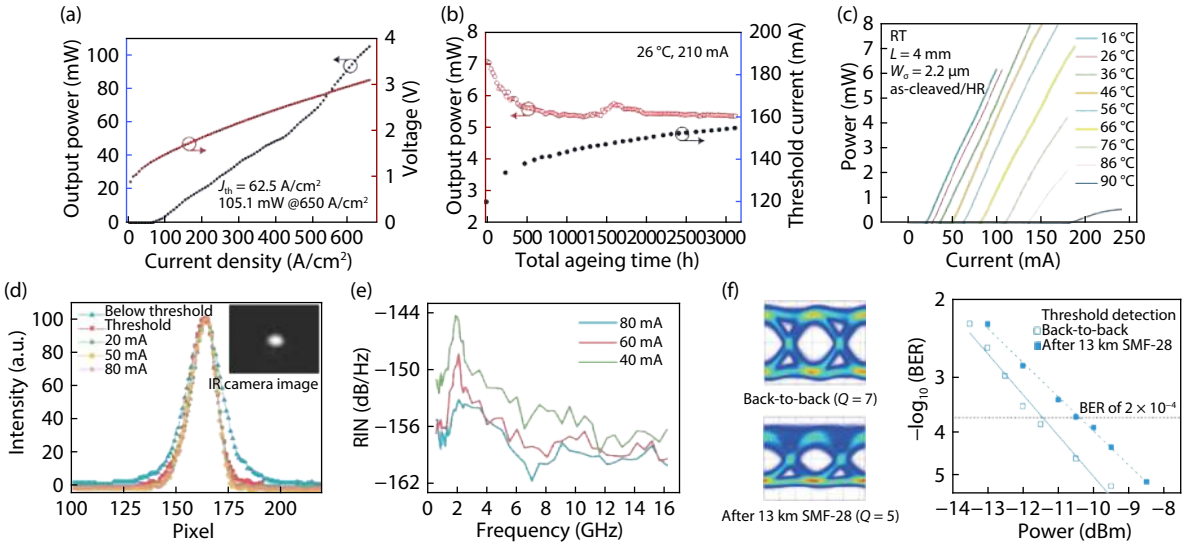

Fig. 4. (Color online) (a) Measured RT CW *L*–*I*–*V* curves for a 50 μm × 3200 μm InAs/GaAs QD laser grown on a Si substrate. (b) Ageing data for the InAs/GaAs QD laser under CW (drive current = 210 mA) at a constant heat sink temperature of 26 °C. (c) Measured CW *L*–*I* curve from a 2.2 μm × 4 mm narrow-ridge-waveguide laser as a function of temperature. (d) Lateral near-field intensity profiles with different injection currents. Inset: infrared (IR) camera image of lasing near-field at the threshold of 20 mA (well above threshold). (e) RIN spectra up to 16 GHz at gain currents of 40, 60 and 80 mA. (f) Experimental results. Left: 25.6 Gb/s eye-diagrams at back-to-back and after transmission over 13 km SMF28. Right: measured bit-error rate (BER) results at different received power. Copyright © 2016, Springer Nature. With permission of Springer (a and b). Reprinted with permission from Ref. [49], The Optical Society (OSA), CC BY 4.0 (c–f).

ties: operating up to 75 °C (120 °C under pulsed operation), with an ultralow threshold current density of 62.5 A/cm^2 and output power of over 100 mW at RT (shown in Fig. 4(a)). It has to be noted that the lifetime of this device is predicted to be over 100, 158 h[11]. These parameters are powerful evidences of the highly reliable and cost competitive Si-based photonic-electronic integration.

Later, the broad-area lasers described in Ref. [11] were used to generate the first gain-switched optical pulses. Their dynamic properties for optical communications have been studied in both experimental and theoretical ways, and good agreement could be found between the two. The typical time duration for the shortest pulses observed is between 175 and 200 ps, with a maximum peak output power of up to 66 mW. A trade-off between maximising the optical power and narrowing the pulse duration has been noticed: a longer high-amplitude drive pulse results in a higher peak optical power, while a shorter one can provide us with a narrower pulse width. Simulations and analysis suggest that there are two main reasons for the broadened pulse width: a limited gain from InAs QDs and a high gain compression factor. Therefore, it is believed that the optical applications of Si-based QD lasers could be significantly improved by increasing the number of active layers, introducing the p-doping in the active region as well as modifying the devices' geometry[50].

Because the multi-transverse-mode operation might limit the laser's dynamic response, the RWG FP lasers with 2.2 μm ridge width were then fabricated to ensure the single-transverse mode lasing at 1.3 μm. In additions, these RWG lasers could help us to take a closer step towards practical applications in tele-/data communications. Depicted in Figs. 4(c)–4(f), the designed RWG QD lasers have a CW threshold current as low as 12.5 mA at RT, and it could operate at up to 90 °C under CW. In addition, an ultra-low relative intensity noise (RIN) (< −150 dB/Hz) was measured in the range of 4–16 GHz. Based on these excellent noise characteristics, 25.6 Gb/s data transmission over 13.5 km SMF-28 has been demonstrated[49]. This low-noise QD laser shows promise for future inter/hyper data-centre interconnection.

Soon after, a comprehensive study was carried out on a 2.5 mm long RWG QD lasers. The small-signal modulation unveils the maximum 3 dB bandwidths of 1.6 GHz with the value of *D*-factors value equals to 0.3 GHz/mA$^{1/2}$, *K*-factors in the range of 2.4 to 3.7 ns and the modulation current efficiencies of 0.4 GHz/mA$^{1/2}$. A simulation of small-signal response was also applied to reveal the optimised device geometry: a 0.75 mm long cavity with 99% and 60% high-reflection coatings and ten QD layers, which forecast a maximum 3 dB-modulation bandwidth of 5 GHz to 7 GHz[51]. More importantly, this work indicates that neither the increased non-radiative recombination in the wetting layer nor the dislocation-induced optical seem to limit the devices' modulation characteristics once the QDs active region provides sufficient gain.

4.2. Distributed-feedback (DFB) lasers on off cut Si substrate

The excellent Si-based III–V FP laser sources with specially designed cavities could implement single-mode lasers, and this will enable wavelength division multiplexing (WDM), which is necessary in high-performance applications[52]. With the development of a selective-area growth technique, high-quality InP-based material directly grown on buffer-free Si substrate was presented in 2014[53]. Based on this technique, the first Si-based InP distributed feedback (DFB) laser array was demonstrated by Wang *et al.* in 2015[54], and the first Si-based O-band DFB array was achieved by the same research group one year later[55]. However, both of them are limited by optical pumping. An electrically pumped DFB laser array on Si substrate was not realised until 2018 when a breakthrough was made by researchers from UCL in the UK and

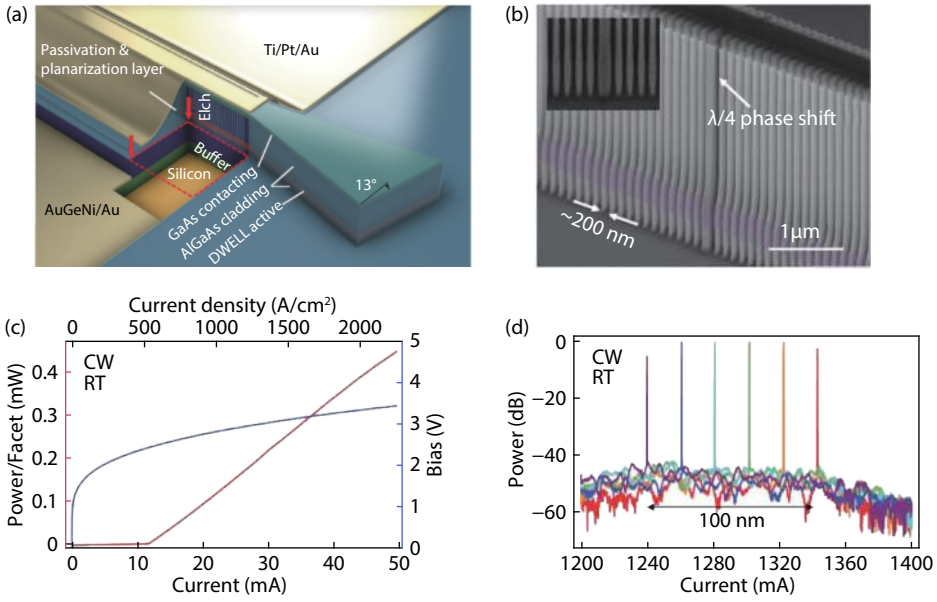

Fig. 5. (Color online) (a) Cutaway schematic of the DFB laser array on Si (not to scale). (b) High-resolution SEM image of the gratings with a $\lambda/4$ phase shift in the middle of the etched gratings. (c) The L–I–V curve of a single 1 mm long Si-based DFB laser. (d) Optical spectra of a DFB laser array with different grating periods around their maximum output power levels before saturation at RT. Reprinted with permission from Ref. [56], The Optical Society (OSA).

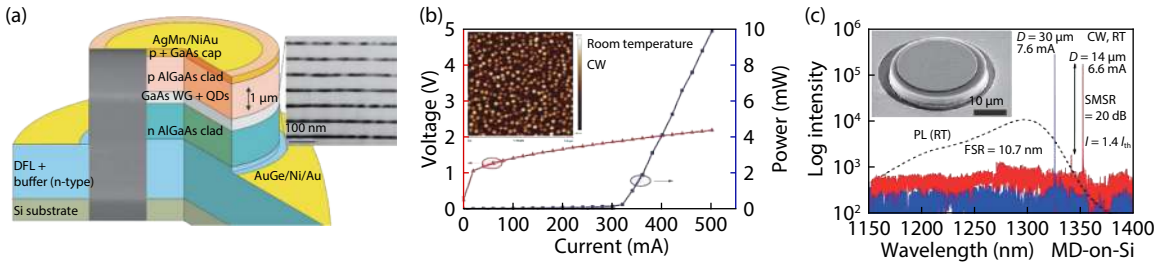

Fig. 6. (Color online) (a) Schematic of layer structure of QD MD laser on Si. The insets are an SEM image of a cross-section of the structure (left) and a TEM image of the QD active region (right). (b) The RT CW L–I–V curve for a 25 μm × 3 mm Si-based edge-emitting QD laser. The inset shows an atomic force microscopy (AFM) image of an uncapped Si-based QD sample. (c) RT CW emission spectrum measured at a current of ~ 1.4 × threshold for MD-on-Si lasers with diameters of 14 and 30 μm. Dashed curve: PL spectrum of QD material (not in scale). The inset: an SEM image of the MD laser (D = 30 μm). Reprinted with permission from Ref. [61], The Optical Society (OSA).

the Sun Yat-sen University in China[56]. An InAs/GaAs QD laser grown on the n-doped Si (001) misoriented 4° towards the [011] plane was used in this work. In addition, the optimised growth conditions yield an almost defect-free active region. Additionally, the conventional complicated regrowth process was replaced by a simpler method, in which lateral surface gratings were fabricated during the waveguide etching process by inductively coupled plasma (ICP). At the same time, the cost-effectively dry-etched anti-reflection (AR) output couplers were utilised to suppress the facet back reflections[57]. The device structure is displayed in Fig. 5 and a $\lambda/4$ phase shift in the middle of the etched gratings can be noted, forcing single-longitudinal-mode lasing in the defect mode[56].

As a result, the first Si-based electrically pumped single-mode DFB laser array using InAs/GaAs QD gain materials was demonstrated, which could lase at RT under CW. The threshold current of this device was as low as 12 mA, and its single-mode side mode suppression ratio (SMSR) was as high as 50 dB[56]. Also, it exhibited a record wavelength coverage of 100 nm, mainly due to the inhomogeneous nature of QDs.

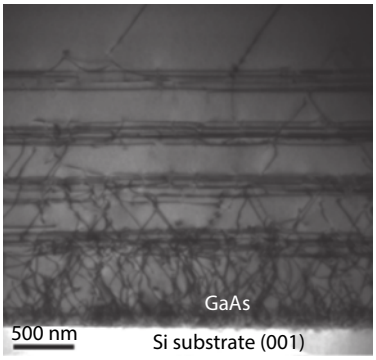

Fig. 7. Bright-field scanning TEM image of on-axis Si (001) substrate.

4.3. Micro-lasers on off cut Si substrate

Not only macro-lasers but also micro-lasers show great potential to work as a long-wavelength light source for Si photonics owing to their short cavity length, small size and low power consumption[58]. Unlike macro-lasers, micro-ring and microdisk (MD) lasers can lock a specific laser wavelength by whispering-gallery-mode (WGM) resonance, which is less sens-

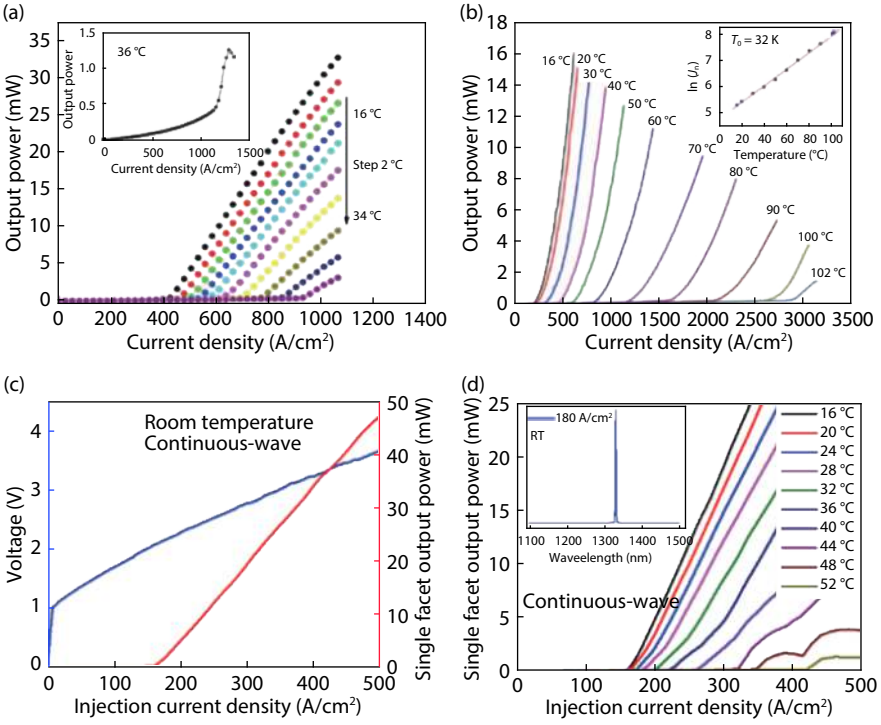

Fig. 8. (Color online) (a) Single-facet output power versus current density for the same Si-based InAs/GaAs QD laser as a function of temperature under CW operation. The inset shows the *L*–*I* curve for this Si-based InAs/GaAs QD laser at a heat sink temperature of 36 °C. (b) Single-facet light power verses current density for an InAs/GaAs QD laser grown on GaAs/Si (001) substrate at various heat sink temperatures under pulsed condition. The inset shows the natural logarithm of current density against temperature in the ranges of 16–102 °C. (c) Measured *L*–*I*–*V* curve of 50 μm × 3 mm broad-area InAs/GaAs QD laser directly grown on GaAs/Si (001) substrate. (d) Measured *L*–*I* curve of InAs/GaAs QD laser directly grown on GaAs/Si (001) as a function of temperature. Inset: lasing spectrum at 180 A/cm^2 injection current density. Reprinted with permission from Ref. [68], CC BY 4.0 (a and b). Reprinted with permission from Ref. [69], CC BY 4.0 (c and d).

itive to temperature variation and thus offers higher stability of emission wavelength[59]. Compared with the micro-ring lasers, the micro-disk lasers attract more attention owing to their better heat dissipation characteristics, as well as their ability to be scaled down to ultra-small diameters (~1 μm)[60].

In 2017, Kryzhanovskaya *et al.* succeeded in demonstrating the first Si-based micro-disk lasers with diameters from 14 to 30 μm and enabled emission in the range of 1320–1350 nm with minima J_{th} of 600 A/cm^2[61]. The layer structure of the fabricated MD laser can be found in Fig. 6(a), and its RT CW light–current–voltage (*L*–*I*–*V*) curve and emission spectrum are shown in Figs. 6(b) and 6(c) respectively. Notably, these devices with a diameter of 30 μm can operate in nearly single-mode up to 60 °C in CW and 110 °C in pulsed mode with a side mode suppression ratio of about 18 dB[62].

5. QD lasers on on-axis Si (001) substrate

Even though, the off cut Si substrate could inhibit the emergence of APBs, adopting the 'exact' (001) Si substrates (shown in Fig. 7) is an essential step to fully exploit the potential of Si photonics because of its compatibility with conventional CMOS processing[63]. There are a few approaches to obtain the III–V lasers on on-axis Si (001) substrates, including the usage of the GaP/Si template[64, 65] and the GaAs-on-V-groove (GoVS) Si template[66, 67]. However, for these technologies, either an intermediate buffer layer or a patterned substrate is needed. To overcome these barriers, Leti developed an APB-free GaAs/Si (001) virtual substrate by using a metal-organic chemical vapour deposition (MOCVD) method, in which a two-step process was used: an initial 40 nm GaAs layer was grown as the nucleation layer that was deposited at low-temperature (400–500 °C), then, a 360 nm GaAs layer was grown in a relative high temperature (600–700 °C)[17]. Subsequently, this grown wafer was transferred to an MBE growth chamber at UCL for the deposition of the rest of the laser structure, which is similar to that described in Section 4, consisting of buffer layers, DFLs, p–i–n structures and the contacting layer.

In this section, our recent achievements in FP and MD QD lasers with on-axis Si (001) substrate will be covered.

5.1. FP lasers on on-axis Si substrate

The first CW electrically pumped InAs/GaAs QD lasers monolithically grown on 'exact' (001) Si substrate were reported by Chen *et al.* from UCL in 2017, in which no intermediate buffer layers or patterned Si substrates were used[68]. In this work, a 600 nm GaAs buffer was first deposited by MBE, followed by five repeats of DFLs and the InAs/GaAs QD laser structure. Finally, this growth process ended with a 300 nm p-type GaAs contact layer. As a result, an RT CW lasing at ~ 1.3 μm with a threshold current density of 425 A/cm^2 and a single-facet output of around 43 mW was achieved (as shown in Fig. 8(a)). Its characteristics under pulsed mode can be seen in Fig. 8(b): it could achieve lasing up to 102 °C with a threshold current density equals to 250 A/cm^2 and a single-facet output power exceeding 130 mW at RT[68].

By optimising the growth conditions, Li *et al.* achieved a high-quality electrically pumped on-axis Si-based QD laser with low threshold current density (160 A/cm^2 @ RT CW).

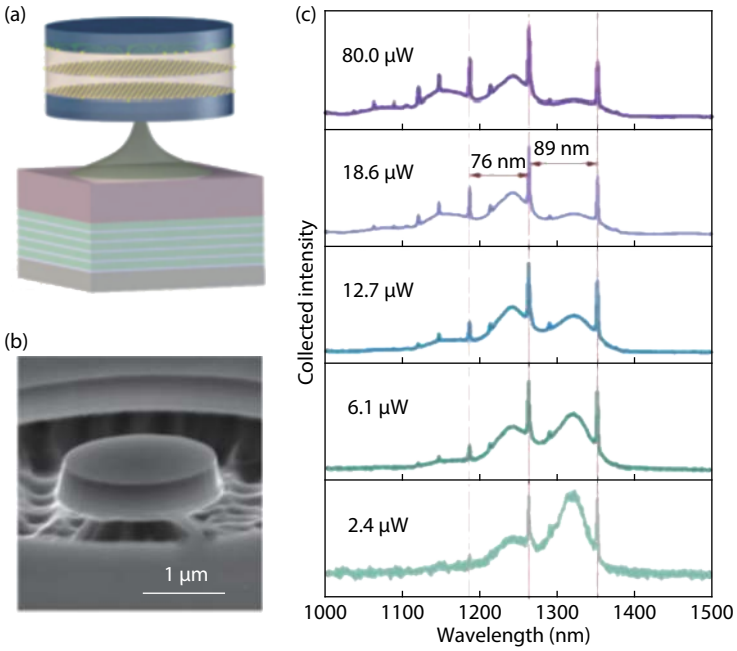

Fig. 9. (Color online) (a) Schematic diagram of a microdisk laser grown on planar on-axis Si (001) substrate. (b) SEM image of a fabricated microdisk laser. (c) Collected PL spectra above and below the lasing threshold of a MD with $D \sim 1.9$ μm. Reprinted with Permission from Ref. [70], The Optical Society (OSA).

Moreover, the lasing was observed at up to 52 °C under CW[69].

5.2. Micro-lasers on on-axis Si substrate

Recently, Zhou *et al.* have developed a CW optically pumped InAs/GaAs QD MD directly grown on on-axis Si (001) substrate[70]. Above the buffer layer, three stacked InAs/$In_{0.15}Ga_{0.85}As$/GaAs dot–in-well (DWELL) active layers were sandwiched by two $Al_{0.4}Ga_{0.6}As$ cladding layers. A 10 nm GaAs layer was used to cap the whole epitaxy structure. Detailed descriptions of the epitaxy structure can be found in Refs. [17, 68].

Fig. 9 displays the schematic diagram of the MD laser together with its SEM image. The lasing characteristics of the fabricated device with small diameter (D) in the range of 1.1–2 μm are demonstrated. According to the measurements, lasing emission from both ground states and excited states were obtained with an ultra-low lasing threshold of ~ 3 μW (for $D \sim 1.1$ μm)[70]. The realisation of on-axis (001) Si-based MD lasers, and their promising lasing characteristics is an essential step towards the high density, large-scale integration of Si photonics.

6. Conclusion

This paper has predominantly reviewed the recent achievements made by UCL in the epitaxial growth of various III–V QD lasers monolithically grown on Si substrates, including the FP laser, the DFB laser and the MD laser. We also discuss material dissimilarity issues between the III–V compounds and Si substrates, which will generate different kinds of defects and seriously hinder the development of Si photonics. The 3-D confined island-structure with discrete energy levels has captured plenty of attention since first realised in 1994 due to its irreplaceable properties in temperature stability and defects immunisation. To obtain a high-performance device, numerous growth techniques have been investigated worldwide, such as the nucleation layers, the dislocation filter layers and the *in situ* thermal annealing process.

Owing to these intense research efforts, 1.3 μm InAs QD lasers monolithically grown on Si (001) substrate with a 4° off-cut towards the [011] plane have achieved impressive results: the FP laser with ultra-low threshold current density (62.5 A/cm^2) and incredibly long life-time (over 100,158 h), the narrow-ridge-waveguide FP laser with excellent noise characteristics (RIN < −150 dB/Hz), and the first electrically pumped DFB laser together with the first Si-based micro-disk laser. However, lasing from the on-axis Si (001) substrate is needed to take advantages of the well-developed CMOS industry. Our group succeeded in realising the first CW electrically pumped InAs/GaAs QD lasers monolithically grown on the on-axis Si (001) substrate lasing up to 102 °C (pulsed) in 2017. Soon after, an improved version was exhibited with a threshold current density of 160 A/cm^2 (@ RT CW) and lasing up to 52 °C under CW mode. Moreover, a MD laser directly grown on 'exact' Si (001) substrate was obtained recently with a lasing threshold as low as 3 μW.

These remarkable accomplishments confirm that the monolithic Si-based QD laser is a promising candidate for integrating the optoelectronics devices with Si platforms and prove the feasibility to fully explore the applications of Si photonics.

Acknowledgements

The authors acknowledge financial support from the UK EPSRC under grant No. EP/P006973/1, and the EPSRC National Epitaxy Facility European project H2020-ICT-PICTURE (780930); the Royal Academy of Engineering (RF201617/16/28) and Investissments d'avenir (IRT Nanoelec: ANR-10-IRT-05 and Need for IoT: ANR-15-IDEX-02). S. Pan and M. Liao thank to the Chinese Scholarship Council for funding their studies. S. Chen acknowledges the Royal Academy of Engineering for funding his Research Fellowship.

References

[1] Reed G T, Mashanovich G, Gardes F Y, et al. Silicon optical modulators. Nat Photonics, 2010, 4, 518

[2] Xiao X, Xu H, Li X Y, et al. High-speed, low-loss silicon Mach–Zehnder modulators with doping optimization. Opt Express, 2013, 21, 4116

[3] Streshinsky M, Ding R, Liu Y, et al. Low power 50 Gb/s silicon traveling wave Mach-Zehnder modulator near 1300 nm. Opt Express, 2013, 21, 30350

[4] Dosunmu O I, Can D D, Emsley M K, et al. High-speed resonant cavity enhanced Ge photodetectors on reflecting Si substrates for 1550-nm operation. IEEE Photonics Technol Lett, 2005, 17, 175

[5] Yin T, Cohen R, Morse M M, et al. 31 GHz Ge n–i–p waveguide photodetectors on silicon-on-insulator substrate. Opt Express, 2007, 15, 13965

[6] Vivien L, Polzer A, Marris-Morini D, et al. Zero-bias 40 Gbit/s germanium waveguide photodetector on silicon. Opt Express, 2012, 20, 1096

[7] Bauters J F, Davenport M L, Heck M J R,et al. Silicon on ultra-low-loss waveguide photonic integration platform. Opt Express, 2013, 21, 544

[8] Heck M J R, Bauters J F, Davenport M L, et al. Ultra-low loss waveguide platform and its integration with silicon photonics. Laser Photon Rev, 2014, 8, 667

[9] Liu H Y, Wang T, Jiang Q, et al. Long-wavelength InAs/GaAs quantum-dot laser diode monolithically grown on Ge substrate. Nat Photonics, 2011, 5, 416

[10] Liang D, Bowers J E. Recent progress in lasers on silicon. Nat Photonics, 2010, 4, 511

[11] Chen S, et al. Electrically pumped continuous-wave III–V quantum dot lasers on silicon. Nat Photonics, 2016, 10, 307

[12] Tanabe K, Watanabe K, Arakawa Y. III–V/Si hybrid photonic devices by direct fusion bonding. Sci Rep, 2012, 2349

[13] Tournié E, Cerutti L, Rodriguez J B, et al. Metamorphic III–V semiconductor lasers grown on silicon. MRS Bull, 2016, 41, 218

[14] Fischer R, Masselink W T, Klem J, et al. Growth and properties of GaAs/AlGaAs on nonpolar substrates using molecular beam epitaxy. J Appl Phys, 1985, 58, 374

[15] Wang W I. Molecular beam epitaxial growth and material properties of GaAs and AlGaAs on Si (100). J Appl Phys, 1984, 44, 1149

[16] Li Q, Lau M. Epitaxial growth of highly mismatched III–V materials on (001) silicon for electronics and optoelectronics. Prog Cryst Growth Charact Mater, 2017, 63, 105

[17] Alcotte R, Martin M, Moeyaert J, et al. Epitaxial growth of antiphase boundary free GaAs layer on 300 mm Si(001) substrate by metalorganic chemical vapour deposition with high mobility. APL Mater, 2016, 4, 46101

[18] Akiyama M, Kawarada Y, Kaminishi K. Growth of single domain gaas layer on (100)-oriented Si substrate by MOCVD. Jpn J Appl Phys, 1984, 23, L843

[19] Norman J C, Jung D, Wan Y, et al. Perspective: The future of quantum dot photonic integrated circuits. APL Photonics, 2018, 3, 30901

[20] Wu J, Chen S, Seeds A, et al. Quantum dot optoelectronic devices: lasers, photodetectors and solar cells. J Phys D, 2015, 48, 363001

[21] Ueda O, Pearton S J. Materials and reliability handbook for semiconductor optical and electron devices. Springer, 2013

[22] Kroemer H. A proposed class of hetero-junction injection lasers. Proc IEEE, 1963, 51, 1782

[23] Alferov Z I. AlAs–GaAs heterojunction injection lasers with a low room-temperature threshold. Sov Phys Semicond, 1970, 3, 1107

[24] Dingle R, Wiegmann W, Henry C H. Quantum states of confined carriers in very thin $Al_xGa_{1-x}As$–GaAs–$Al_xGa_{1-x}As$ heterostructures. Dordrecht: Springer, 1988, 173

[25] Kapon E, Simhony S, Bhat R, et al. Single quantum wire semiconductor lasers. Appl Phys Lett, 1989, 55, 2715

[26] Arakawa Y, Sakaki H. Multidimensional quantum well laser and temperature dependence of its threshold current. Appl Phys Lett, 1982, 40, 939

[27] Kirstaedter N, Ledentsov N N, Grundmann M, et al. Low threshold, large To injection laser emission from (InGa)As quantum dots. Electron Lett, 1994, 30, 1416

[28] Nishi K, Takemasa K, Sugawara M, et al. Development of quantum dot lasers for data-com and silicon photonics applications. IEEE J Sel Top Quantum Electron, 2017, 23, 1

[29] Nishi K, Kageyama T, Yamaguchi M, et al. Molecular beam epitaxial growths of high-optical-gain InAs quantum dots on GaAs for long-wavelength emission. J Cryst Growth, 2013, 378, 459

[30] Ilahi B, Souaf M, Baira M, et al. Evolution of InAs/GaAs QDs size with the growth rate: a numerical investigation. J Nanomater, 2015, 2015, 1

[31] Leonard D, Fafard S, Pond K, et al. Structural and optical properties of self-assembled InGaAs quantum dots. J Vac Sci Technol B, 1994, 12, 2516

[32] Nishi K, Saito H, Sugou S, et al. A narrow photoluminescence linewidth of 21 meV at 1.35 μm from strain-reduced InAs quantum dots covered by $In_{0.2}Ga_{0.8}As$ grown on GaAs substrates. Appl Phys Lett, 1999, 74, 1111

[33] Otsubo K, Hatori N, Ishida M, et al. Temperature-insensitive eye-opening under 10-Gb/s modulation of 1.3-μm P-doped quantum-dot lasers without current adjustments. Jpn J Appl Phys, 2004, 43, L1124

[34] Takada K, Tanaka Y, Matsumoto T, et al. Wide-temperature-range 10.3 Gbit/s operations of 1.3 μm high-density quantum-dot DFB lasers. Electron Lett, 2011, 47, 206

[35] CapuaA, et al. Direct correlation between a highly damped modulation response and ultra low relative intensity noise in an InAs/GaAs quantum dot laser. Opt Express, 2007, 15, 5388

[36] Jung D, Zhang Z, Norman J, et al. Highly reliable low-threshold inas quantum dot lasers on on-axis (001) Si with 87% injection efficiency. ACS Photonics, 2018, 5, 1094

[37] Ovid'ko I. Relaxation mechanisms in strained nanoislands. Phys Rev Lett, 2002, 88, 46103

[38] Tillmann K, Förster A. Critical dimensions for the formation of interfacial misfit dislocations of $In_{0.6}Ga_{0.4}As$ islands on GaAs(001). Thin Solid Films, 2000, 368, 93

[39] Mi Z, Yang J, Bhattacharya P, et al. High-performance quantum dot lasers and integrated optoelectronics on Si. Proc IEEE, 2009, 97, 1239

[40] Shi B, Li Q, Lau K M. Self-organized InAs/InAlGaAs quantum dots as dislocation filters for InP films on (001) Si. J Cryst Growth, 2017, 464, 28

[41] Linder K, Phillips J, Qasaimeh O, et al. Self-organized $In_{0.4}Ga_{0.6}As$ quantum-dot lasers grown on Si substrates. Appl Phys Lett, 1999, 70(10), 1355

[42] Wang T, Liu H, Lee A, et al. 1.3-μm InAs/GaAs quantum-dot lasers monolithically grown on Si substrates. Opt Express, 2011, 19, 11381

[43] Lee A D, Jiang Q, Tang M C, et al. InAs/GaAs quantum-dot lasers monolithically grown on Si, Ge, and Ge-on-Si substrates. IEEE J Sel Top Quantum Electron, 2013, 19, 1901107

[44] Chen S M, Tang M, Wu J, et al. 1.3-μm InAs/GaAs quantum-dot lasers monolithically grown on Si substrates using InAlAs/GaAs dislocation filter layers. Opt Express, 2014, 22, 11528

[45] Orchard J R, Shutts S, Sobiesierski A, et al. In situ annealing enhancement of the optical properties and laser device performance of InAs quantum dots grown on Si substrates. Opt Express, 2016, 24, 6196

[46] Jiang Q, Tang M C, Wu J, et al. 1.3 μm InAs/GaAs quantum-dot laser monolithically grown on Si substrates operating over 100

°C. Electron Lett, 2014, 50, 1467
[47] Liao M, Chen S, Park J S, et al. III–V quantum-dot lasers monolithically grown on silicon. Semicond Sci Technol, 2018, 33, 123002
[48] Tang M, Chen S M, Wu J, et al. Optimizations of defect filter layers for 1.3-μm InAs/GaAs quantum-dot lasers monolithically grown on Si substrates. IEEE J Sel Top Quantum Electron, 2016, 22, 50
[49] Liao M, Chen S M, Liu Z X, et al. Low-noise 13 μm InAs/GaAs quantum dot laser monolithically grown on silicon. Photonics Res, 2018, 6, 1062
[50] Hantschmann C, Vasil'ev P P, Chen S M, et al. Gain switching of monolithic 1.3 μm InAs/GaAs quantum dot lasers on silicon. J Light Technol, 2018, 36, 3837
[51] Hantschmann C, Vasil'ev P P, Wonfor A, et al. Understanding the bandwidth limitations in monolithic 1.3 μm InAs/GaAs quantum dot lasers on silicon. J Light Technol, 2019, 37, 949
[52] Agrawal G P. Fiber-optic communication systems. Wiley, 2013
[53] Merckling C, Waldron N, Jiang S, et al. Heteroepitaxy of InP on Si(001) by selective-area metal organic vapor-phase epitaxy in sub-50 nm width trenches: The role of the nucleation layer and the recess engineering. J Appl Phys, 2014, 115, 23710
[54] Wang Z, Tian B, Pantouvaki M, et al. Room-temperature InP distributed feedback laser array directly grown on silicon. Nat Photonics, 2015, 9, 837
[55] Tian B, Wang Z C, Pantouvaki M, et al. Room temperature O-band DFB laser array directly grown on (001) silicon. Nano Lett, 2017, 17, 559
[56] Wang Y, Chen S M, Yu Y, et al. Monolithic quantum-dot distributed feedback laser array on silicon. Optica, 2018, 5, 528
[57] Kim H C, Wiedmann J, Matsui K, et al. 1.5-μm-wavelength distributed feedback lasers with deeply etched first-order vertical grating. Jpn J Appl Phys, 2001, 40, L1107
[58] Vahala K J. Optical microcavities. Nature, 2003, 424, 839
[59] Maximov M V, Kryzhanovskaya N V, Nadtochiy A M, et al. Ultrasmall microdisk and microring lasers based on InAs/InGaAs/GaAs quantum dots. Nanoscale Res Lett, 2014, 9, 657
[60] Kryzhanovskaya N V, Zhukov A Z, Maximov M V, et al. Room temperature lasing in 1-μm microdisk quantum dot lasers. IEEE J Sel Top Quantum Electron, 2015, 21, 709
[61] Kryzhanovskaya N, Zhukov A E, Maximov M V, et al. Heat-sink free CW operation of injection microdisk lasers grown on Si substrate with emission wavelength beyond 13 μm. Opt Lett, 2017, 42, 3319
[62] Kryzhanovskaya N, Moiseev E, Polubavkina Y, et al. Elevated temperature lasing from injection microdisk lasers on silicon. Laser Phys Lett, 2018, 15, 15802
[63] Volz K, Beyer A, Witte W, et al. GaP-nucleation on exact Si (001) substrates for III/V device integration. J Cryst Growth, 2011, 315, 37
[64] Liu A Y, Peters J, Huang X, et al. Electrically pumped continuous-wave 13 μm quantum-dot lasers epitaxially grown on on-axis (001) GaP/Si. Opt Lett, 2017, 42, 338
[65] Jung D, Song Y, Lee M, et al. InGaAs/GaAs quantum well lasers grown on exact GaP/Si (001). Electron Lett, 2014, 50, 1226
[66] Li Q, Ng K W, Lau K M. Growing antiphase-domain-free GaAs thin films out of highly ordered planar nanowire arrays on exact (001) silicon. Appl Phys Lett, 2015, 106, 72105
[67] Li Q, Wan Y T, Liu A Y, et al. 13-μm InAs quantum-dot micro-disk lasers on V-groove patterned and unpatterned (001) silicon. Opt Express, 2016, 24, 21038
[68] Chen S M, Liao M Y, Tang M C, et al. Electrically pumped continuous-wave 1.3 μm InAs/GaAs quantum dot lasers monolithically grown on on-axis Si (001) substrates. Opt Express, 2017, 25, 4632
[69] Li K, Liu Z, Tang M, et al. O-band InAs/GaAs quantum dot laser monolithically integrated on exact (001) Si substrate. J Cryst Growth, 2019, 511, 56
[70] Zhou T J, Tang M C, Xiang G H, et al. Ultra-low threshold InAs/GaAs quantum dot microdisk lasers on planar on-axis Si (001) substrates. Optica, 2019, 6, 430